

## Methanolysis of *Jatropha curcas* oil using $K_2CO_3/CaO$ as a solid base catalyst

Gajanan SAHU<sup>1,\*</sup>, Sujan SAHA<sup>1</sup>, Sudipta DATTA<sup>1</sup>, Prakash CHAVAN<sup>1</sup>, Satyanarayan NAIK<sup>2</sup>

<sup>1</sup>Gasification and Liquefaction Research Group, Central Institute of Mining and Fuel Research, CSIR, Dhanbad, Jharkhand, India

<sup>2</sup>Centre for Rural Development and Technology, Indian Institute of Technology Delhi, Hauz Khas, New Delhi, India

Received: 04.01.2017

Accepted/Published Online: 09.05.2017

Final Version: 20.12.2017

**Abstract:** Biodiesel, fatty acid methyl ester produced by the transesterification of vegetable oil with methanol, is a promising alternative to petroleum-based diesel fuel. In the present study, the methanolysis of high free fatty acid (FFA) *Jatropha curcas* oil in a transesterification reaction using  $K_2CO_3/CaO$  solid base catalyst was studied. The various reaction parameters in the transesterification reaction were also discussed. The catalyst was characterized by means of Fourier transform infrared, X-ray diffraction, temperature programmed desorption of  $CO_2$ , scanning electron microscopy, particle size analyzer, true density, and surface area analyzer. The optimum conversion of jatropha oil was 92% when the transesterification reaction was carried out at 70 °C with 10:1 molar ratio of methanol to oil at reaction time of 3 h and catalyst amount of 6 wt%. The efficiency of catalysts in the methanolysis of jatropha oil was also investigated.

**Key words:** Transesterification, jatropha oil, solid base catalyst, biodiesel,  $K_2CO_3/CaO$

### 1. Introduction

The development of modern day society is attributed to mainly fossil fuel application as man has reduced distances by means of modern transport facilities. The transport facilities are mainly dependent upon the petroleum product derived from fossil fuel. The uses of fossil fuel are not free from concerns or risks such as exhaustible gaseous products as a result posing a great threat to the environment by releasing  $CO_2$  into the atmosphere due to burning of large scale fuel in IC engines as well as plants and factories. In order to save our green planet from the hazards of burning of fossil fuel, the scientific community is forced to search for new renewable, sustainable, ecofriendly fuels to meet the demands of automobiles.<sup>1</sup>

Several rural technologies in respect of extraction and use of energy are focused on in India such as cow dung, oils from jatropha, karanja, neem, and castor, etc. These oil seed-producing plants are widespread throughout the length and breadth of the country. The growing of these plants does not require much care and expenditure and they produce very good seeds rich in oil contents.<sup>2</sup> It is in the interest of the scientific community to look for alternative sources of fuel from these plants. Out of these plants, jatropha is an oil seed-bearing plant pandemic in India. These plants can grow almost everywhere. It holds tremendous potential for the supply of nonedible oil if research is carried out in the right direction.

Methanolysis is a process in which vegetable oil is transesterified with methanol in the presence of homogeneous acid or base catalysts. Sulfuric acid and hydrochloric acid are commonly used as acid catalysts; however, the reaction time is very long and a high molar ratio of methanol to oil is required. NaOH, KOH,

\*Correspondence: [gajanansahu@gmail.com](mailto:gajanansahu@gmail.com)

sodium alkoxide, and potassium alkoxides are used as base catalysts for the transesterification reaction.<sup>3</sup> As the catalytic activity of a base is greater than that of acid and acid catalyst is more corrosive to the reaction vessel, the base catalyst is preferred for the transesterification reaction. However, in the conventional homogeneous route, the removal of catalyst from the reaction product is very difficult and a large amount of waste water is produced to separate the biodiesel from the reaction mixture. Therefore, our concentration is going to develop environmentally friendly heterogeneous catalysts due to the reduction of environmental degradation and easy separation of catalyst from the reaction product. Few studies about transesterification of vegetable oils including *Jatropha curcas* oil (JCO) by using CaO-based catalysts have been reviewed. Mixture of active solid base and  $\text{Fe}_2(\text{SO}_4)_3$  solid acid catalysts have been used for biodiesel production from JCO having high FFA in a single step simultaneous esterification and transesterification process.<sup>4</sup>  $\text{K}_2\text{CO}_3/\text{CaO}$  catalyst has been used for the transesterification of canola oil with methanol.<sup>5</sup> Degirmenbasi et al. reported that the  $\text{K}_2\text{O}$  species or Ca–O–K groups are the active sites of catalyst on which the methoxide ions are formed and it attacks the carbonyl carbon of triglycerides to get more methyl esters.<sup>5</sup> The solid super base calcium oxide has been prepared by dipping in ammonium carbonate followed by calcinations at  $900\text{ }^\circ\text{C}$  for transesterification of JCO.<sup>6</sup> Lithium nitrate loaded on calcium oxide has been used as solid catalyst for the transesterification of jatropha oil containing 8.3 wt% of FFA.<sup>7</sup> Transesterification of JCO to biodiesel was studied by using CaO–MgO mixed metal oxides with different Ca/Mg atomic ratios. Around 90% of FAME was obtained using CM0.5 catalyst under the optimum reaction condition: 3 h reaction time, 25:1 methanol to oil molar ratio, 3 wt% catalysts loading, and  $120\text{ }^\circ\text{C}$  reaction temperature. Brunauer–Emmett–Teller (BET), X-ray diffraction (XRD), scanning electron microscopy (SEM), and temperature programmed desorption (TPD) methods are used for catalyst characterization.<sup>8</sup> CaO–MgO mixed oxide catalyst was employed for biodiesel production by the transesterification of jatropha oil. The experimental results indicated that the CaO–MgO catalyst gave a 93.55% yield of FAME at  $115.87\text{ }^\circ\text{C}$ , 3.44 h reaction time, 3.70 wt% of catalyst amount, and 38.67:1 methanol/oil molar ratio.<sup>9</sup> Calcium-based mixed oxide catalysts (CaMgO and CaZnO) have been reported for methanolysis of JCO to biodiesel.<sup>10</sup> Methanolysis of JCO was carried out in the presence of ash generated from palm empty fruit bunch (EFB) as a heterogeneous catalyst.<sup>11</sup> The methanolysis of sunflower oil using alkaline and alkaline-earth metal compounds as catalysts has been reported. The results indicated the catalytic activity of alkaline earth metal compounds is controlled by a balance between solubility, basic strength, and specific surface area (SA) of the solid catalysts.<sup>12</sup> Potassium compounds loaded on calcium oxide-supported catalyst have been prepared for studying the transesterification of Chinese tallow seed oil with methanol.<sup>13</sup> The activity of activated CaO as a catalyst has been studied in the production of biodiesel by the transesterification of sunflower oil with methanol.<sup>14</sup> Biodiesel synthesis from sunflower oil has been studied by using CaO as a heterogeneous catalyst.<sup>15</sup> The methanolysis of sunflower oil has been studied by using alumina/silica-supported  $\text{K}_2\text{CO}_3$  as a heterogeneous catalyst. Experimental results have shown that more than 93% conversion of vegetable oil to fatty acid methyl ester (FAME) was achieved with optimal reaction conditions of methanol to oil molar ratio of 15:1, reaction temperature  $120\text{ }^\circ\text{C}$ , and 2 wt% catalyst used. Catalyst characterization revealed that the  $\text{K}_2\text{CO}_3$  present on the catalyst surface was the only active component in the reaction mixture.<sup>16</sup> The active phase of calcium oxide has been proved as a solid base catalyst for the transesterification of soybean oil with methanol. The results showed that calcium diglyceride was the active phase in the catalytic reaction using calcium oxide for biodiesel production.<sup>17</sup> The application of  $\text{KNO}_3/\text{CaO}$  catalyst in the reaction of triglycerides with methanol has been studied. The maximum conversion of 98% has been achieved under the optimum reaction condition.<sup>18</sup> Methanolysis of soybean oil was carried

out in the presence of CaO, Ca(OH)<sub>2</sub>, and CaCO<sub>3</sub>. Around 93% yield of FAME was obtained using CaO as a solid base catalyst for 1 h reaction time.<sup>19</sup> K<sub>2</sub>CO<sub>3</sub> supported on MgO has been selected as a highly efficient catalyst for the preparation of biodiesel from soybean oil.<sup>20</sup> CaO was used as a solid base catalyst for the transesterification of soybean oil with methanol. The biodiesel yield of 95% was obtained under the reaction condition of 12:1 methanol to oil molar ratio, 8% CaO catalyst at 65 °C. It has been also remarked that the lifetime of catalyst was longer than that of calcined K<sub>2</sub>CO<sub>3</sub>/γ-Al<sub>2</sub>O<sub>3</sub>, KF/γ-Al<sub>2</sub>O<sub>3</sub>.<sup>21</sup> K<sub>2</sub>CO<sub>3</sub>/Al<sub>2</sub>O<sub>3</sub> was demonstrated as a solid base catalyst for transesterification of triolein with methanol.<sup>22</sup>

In this paper, the novelty of this work is to develop a K<sub>2</sub>CO<sub>3</sub>/CaO solid base catalyst for biodiesel synthesis from transesterification of high FFA JCO. Although there are some publications about K<sub>2</sub>CO<sub>3</sub>/CaO solid based catalyst using transesterification of vegetable oils, none of them is related to high FFA JCO. The maximum conversion of jatropha oil to methyl ester was also reported. FTIR, true density, BET SA, XRD, CO<sub>2</sub>-TPD, and a particle size analyzer were used for the catalyst characterization. The influence of the reaction parameters such as molar ratio of methanol to oil, reaction time, and the catalyst amount on the conversion of jatropha oil was also investigated.

## 2. Results and discussion

The true density, apparent density, and porosity of CaO and K<sub>2</sub>CO<sub>3</sub>/CaO are depicted in Table 1. It may be seen that the porosity value of CaO and 35% K<sub>2</sub>CO<sub>3</sub>/CaO catalysts were 20.83% and 18.60%, respectively. The decrease in the porosity value of K<sub>2</sub>CO<sub>3</sub>/CaO catalyst may be due to blocking of pores by the active metal constituent.

**Table 1.** True density, apparent density, and porosity of solid base catalysts.

Catalysts	True density	Apparent density (g/cm <sup>3</sup> )	Porosity (%)
35% K <sub>2</sub> CO <sub>3</sub> /CaO	2.57	2.09	18.60
CaO	2.68	2.12	20.83

SA, pore volume, pore diameter of prepared catalyst, and CaO support are presented in Table 2; 35% K<sub>2</sub>CO<sub>3</sub>/CaO catalyst has a SA of 6.67 m<sup>2</sup>/g and a pore diameter of 144 Å. These values are higher than those of the pure CaO catalyst. The increase in SA with loading amount of K<sub>2</sub>CO<sub>3</sub> may be due to the much higher pore volume or opening of closed pores on the surface of the catalyst during calcinations.

**Table 2.** BET SA, pore volume, and pore diameter of different catalysts.

Catalysts	Surface area SA <sub>BET</sub> (m <sup>2</sup> /g)	Pore volume V <sub>pore</sub> (cm <sup>3</sup> /g)	Pore diameter D <sub>pore</sub> (Å)
35% K <sub>2</sub> CO <sub>3</sub> /CaO	6.67	0.024	144.0
CaO	3.48	0.0082	94.9

The FTIR spectra of the (a) 35% K<sub>2</sub>CO<sub>3</sub>/CaO and (b) CaO catalysts are shown in Figure 1. The absorption band at 3444 cm<sup>-1</sup> in CaO could be assigned to the presence of OH stretching bands. Moreover, 35% K<sub>2</sub>CO<sub>3</sub>/CaO catalyst showed an absorption band at 3434 cm<sup>-1</sup> that could be ascribed to the OH stretching bands.<sup>11</sup> The bands at 1435.25 cm<sup>-1</sup> and 867.58 cm<sup>-1</sup> in K<sub>2</sub>CO<sub>3</sub>/CaO correspond to the C–O bond.<sup>23</sup> The

wide and strong bands at around  $418\text{ cm}^{-1}$  and  $578\text{ cm}^{-1}$  in  $\text{K}_2\text{CO}_3/\text{CaO}$  correspond to Ca–O bonds.<sup>23</sup> The peak at around  $1783.92\text{ cm}^{-1}$  in  $\text{K}_2\text{CO}_3/\text{CaO}$  may be due to the  $\text{K}_2\text{CO}_3$  group.<sup>23</sup> The FTIR peak position at  $3644.77\text{ cm}^{-1}$  indicates the presence of a surface hydroxyl group. Furthermore, another peak on 35%  $\text{K}_2\text{CO}_3/\text{CaO}$  at  $3696\text{ cm}^{-1}$  is responsible for the presence of an isolated OH group. This isolated OH group becomes responsible for active catalytic activity. Our above observation finds support from the work by Granados et al.<sup>14</sup> They conducted biodiesel formation from sunflower oil using calcium oxide catalyst. This group found a hydroxyl band in the FTIR spectrum at  $3647\text{ cm}^{-1}$  and  $3572\text{ cm}^{-1}$  and it was assigned to the OH group of  $\text{Ca}(\text{OH})_2$ . They also got a band at  $3736\text{ cm}^{-1}$  and it was assigned to the isolated OH group. This active compound is arising from the support site.

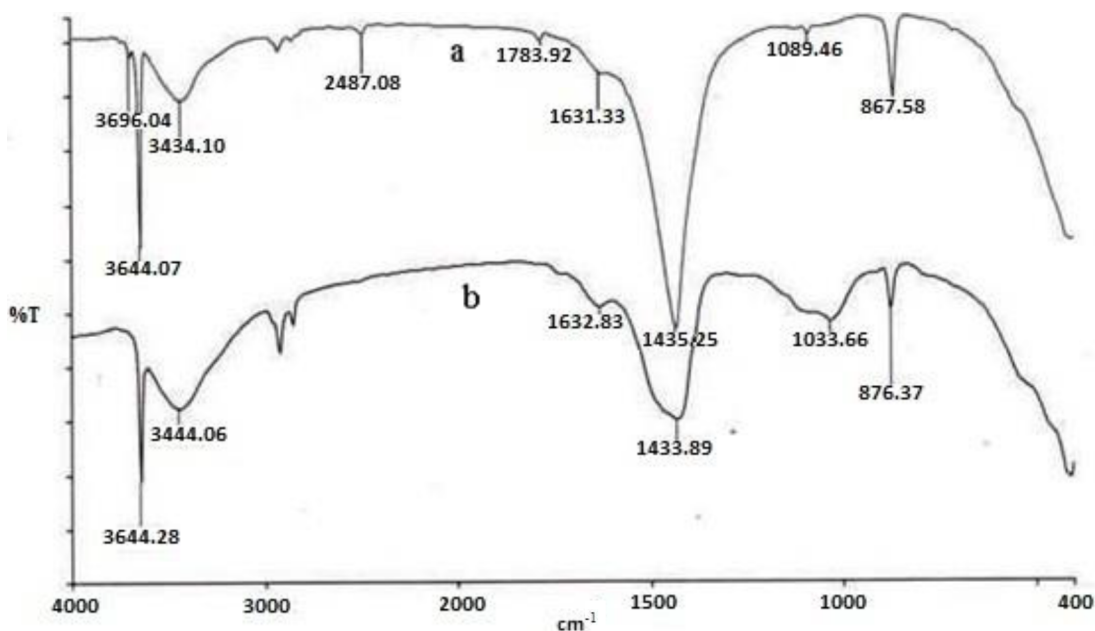
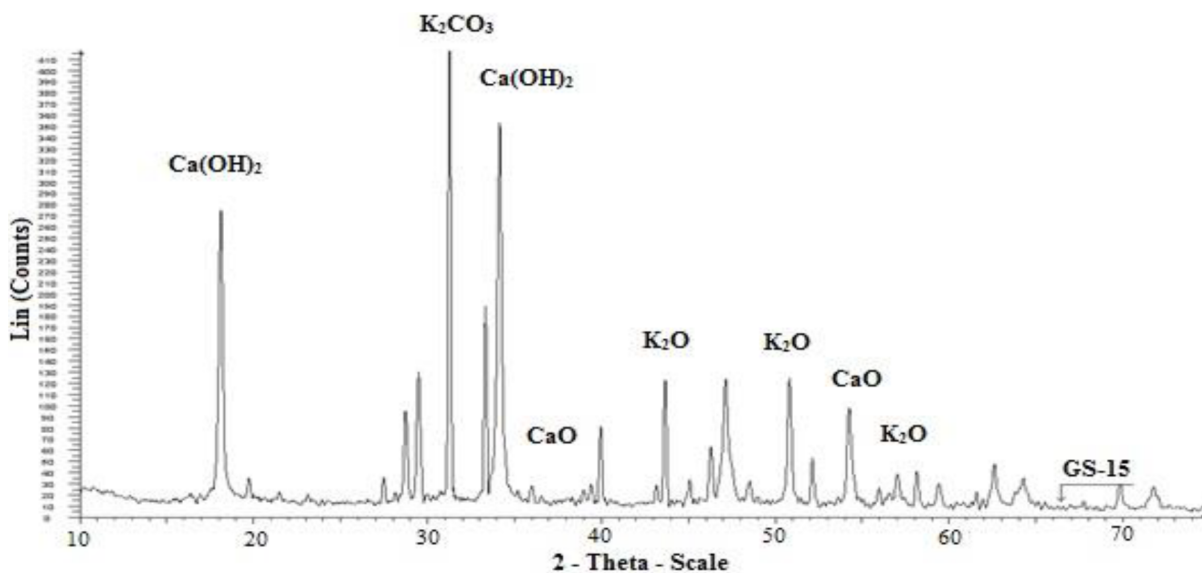
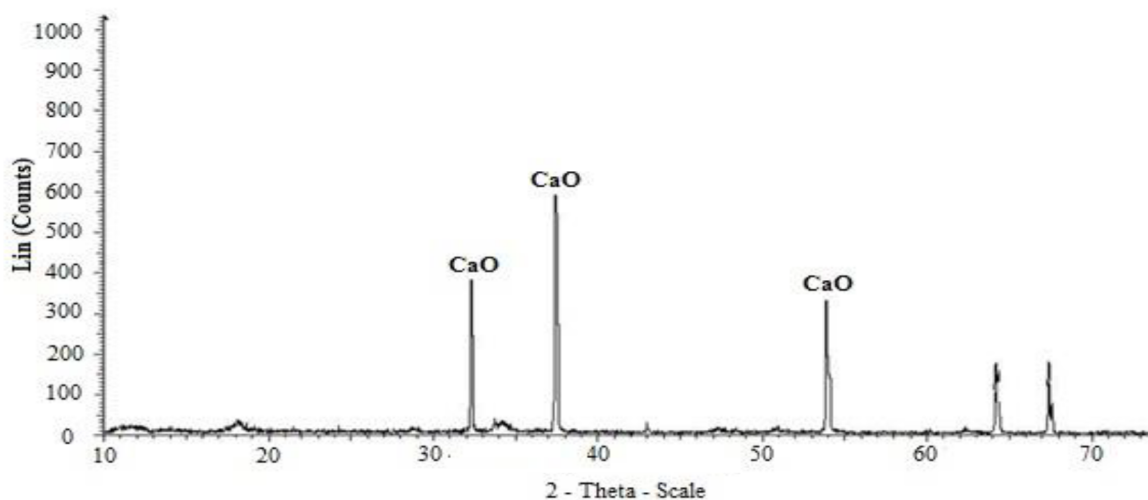


Figure 1. FTIR spectra of (a) 35%  $\text{K}_2\text{CO}_3/\text{CaO}$  and (b)  $\text{CaO}$ .

The powdered XRD patterns of calcined (a) 35%  $\text{K}_2\text{CO}_3/\text{CaO}$  catalyst and (b) pure  $\text{CaO}$  are illustrated in Figure 2. Lime, portlandite, and calcite phases were present in the XRD spectra of  $\text{CaO}$ . The  $2\theta$  angle of the phases was  $18.02^\circ$  and  $34.08^\circ$  of  $\text{Ca}(\text{OH})_2$ , and  $32.1^\circ$ ,  $37.2^\circ$ , and  $54^\circ$  of  $\text{CaO}$  observed in  $\text{CaO}$  catalyst. The calcined 35%  $\text{K}_2\text{CO}_3/\text{CaO}$  catalyst showed peaks at  $31.30^\circ$  due to the presence of monoclinic  $\text{K}_2\text{CO}_3$ .<sup>24</sup> The characteristic peaks at  $2\theta$  of  $18.16^\circ$ ,  $34^\circ$ , and  $47.18^\circ$  due to  $\text{Ca}(\text{OH})_2$  (portlandite) were observed. This is formed due to partly hydration of fresh  $\text{CaO}$ . The new diffraction peaks at  $31^\circ$ ,  $45^\circ$ , and  $58^\circ$  were assigned to the trigonal butschliite. The peaks at  $23^\circ$ ,  $36.44^\circ$ , and  $40^\circ$  were assigned to the presence of  $\text{CaCO}_3$  (calcite). The peaks observed at  $2\theta$  of  $43.4^\circ$ ,  $51.24^\circ$ , and  $57.70^\circ$  were due to the presence of  $\text{K}_2\text{O}$  species formed during calcinations.<sup>5</sup> Butschliite is mainly composed of  $\text{K}_2\text{O}$ ,  $\text{CaO}$ , and  $\text{CO}_2$ . Sharp and highly intense peaks of calcined catalyst observed in the XRD define the well crystallized structure of the catalyst.<sup>25</sup> The  $\text{K}_2\text{O}$  species or the Ca–O–K group obtained from partial decomposition of the  $\text{K}_2\text{CO}_3$  and  $\text{K}_2\text{CO}_3$  were the main active components that increased the catalytic activity of the catalyst. The crystallite size of catalysts can be calculated from the full width at half maximum (FWHM) of corresponding peaks (the most intense peaks) by means of the Scherrer equation. The equation is given below:<sup>10</sup>

(a) 35% K<sub>2</sub>CO<sub>3</sub>/CaO

(b) CaO

**Figure 2.** XRD spectra of (a) 35% K<sub>2</sub>CO<sub>3</sub>/CaO and (b) CaO.

$$t = \frac{0.89\lambda}{\beta_{hkl} \cos \theta_{hkl}} \quad (1)$$

where  $t$  is the crystallite size for (hkl) phase (nm),  $\lambda$  is the X-ray wavelength of radiation for CuK $\alpha$ ,  $\beta_{hkl}$  is the FWHM at (hkl) peak in radian, and  $\theta$  is the diffraction angle for (hkl) phase.

The crystallite sizes for 35% K<sub>2</sub>CO<sub>3</sub>/CaO, CaO were 254 and 568 nm, respectively. However, the crystallite sizes of catalysts were just the reverse order of catalyst's SA. Thus, the results indicated that the crystal sizes of catalysts were in agreement with the SA analysis. These larger crystallite sizes of CaO gave lower SA, which could be involved in some external/internal diffusion restrictions as compared to 35% K<sub>2</sub>CO<sub>3</sub>/CaO catalyst.

The CO<sub>2</sub>-TPD profiles of (a) 35% K<sub>2</sub>CO<sub>3</sub>/CaO catalyst and (b) CaO are presented in Figure 3. The first two desorption peaks at 238.1 °C and 327.1 °C can be ascribed to the weak basic sites present in the 35% K<sub>2</sub>CO<sub>3</sub>/CaO catalyst. Another peak located at 409.3 °C indicated the existence of medium basic sites.<sup>26</sup> The last two desorption peaks at 618.2 °C and 720.3 °C could be due to the interaction of CO<sub>2</sub> with strong basic sites of the catalyst. However, in the case of CaO support, two desorption peaks appeared at 339.3 °C and 421.9 °C due to the presence of weak and medium basic sites of the catalyst. A strong basic strength corresponded to Ca<sup>2+</sup>-O<sup>2-</sup> pairs that appeared at 568 °C.<sup>8</sup> Taufiq-Yap et al., Shumaker et al., and Cosimo et al. have reported the weak basic sites correspond to OH<sup>-</sup> groups on the surface, the medium strength sites are related to Mg<sup>2+</sup>-O<sup>2-</sup> and Al<sup>3+</sup>-O<sup>2-</sup> pairs, and the strong basic sites correspond to isolated O<sup>2-</sup> anion.<sup>8,27,28</sup> In the present study, weak basic sites corresponded to the OH<sup>-</sup> group on the surface, the medium strength sites were related to Ca<sup>2+</sup>-O<sup>2-</sup>, and the strong basic site was related to isolated O<sup>2-</sup> anions. The basic sites and total amount of catalyst basicity are depicted in Table 3. From Table 3, it is observed that the basicity of 35% K<sub>2</sub>CO<sub>3</sub>/CaO catalyst was lower than that of CaO. The catalytic activity of 35% K<sub>2</sub>CO<sub>3</sub>/CaO catalyst was greater than that of CaO. The lower catalytic activity of CaO may be due to the low SA of CaO, which could have involved some diffusion control between the reactant and the basic active sites located inside the pores of the CaO catalyst. Taufiq-Yap et al. have reported the same result in the case of catalytic activity of CM0.5 and CM8.<sup>8</sup> The catalytic activity of CM8 was lower than that of CM0.5, although the highest level of basicity was observed in CM8. The fall in the catalytic activity of CM8 was due to the low SA.

**Table 3.** Basic sites and basicity of solid base catalysts.

Catalysts	35% K <sub>2</sub> CO <sub>3</sub> /CaO	CaO
CO <sub>2</sub> -TPD	Weak, medium, strong basic sites	Weak, medium, strong basic sites
Basicity (μmol/g)	85.50	201.64

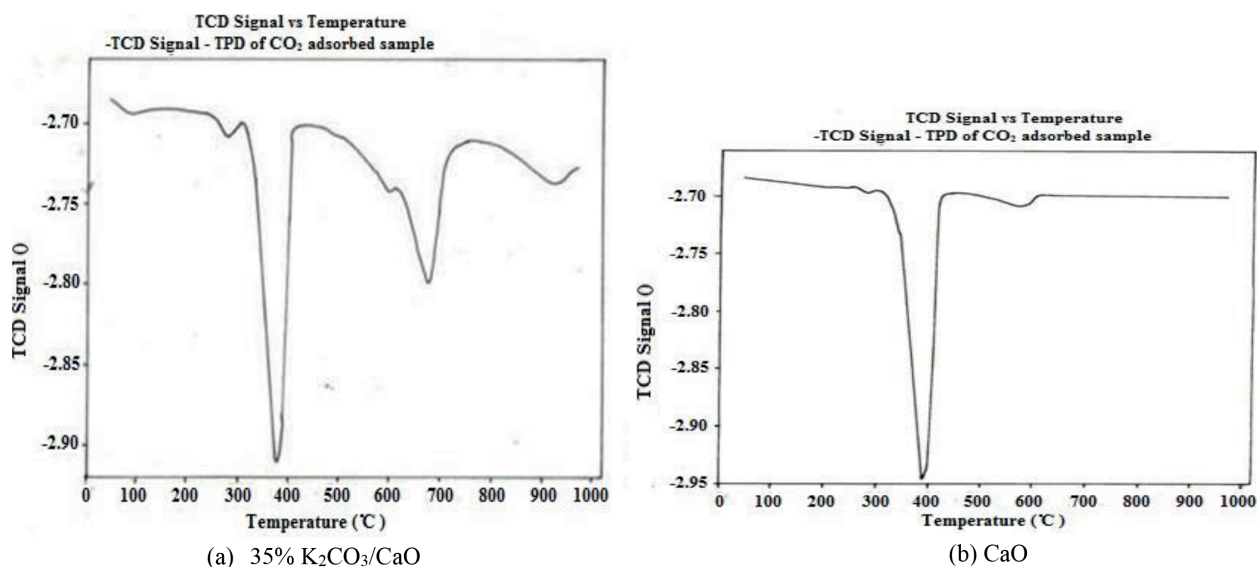


**Figure 3.** CO<sub>2</sub>-TPD of (a) 35% K<sub>2</sub>CO<sub>3</sub>/CaO and (b) CaO.

The SEM micrographs of 35% K<sub>2</sub>CO<sub>3</sub>/CaO catalyst at different magnifications are shown in Figures 4a–4d). Most of the catalyst particles were within 1–114 μm in size, porous with irregular shape. This result

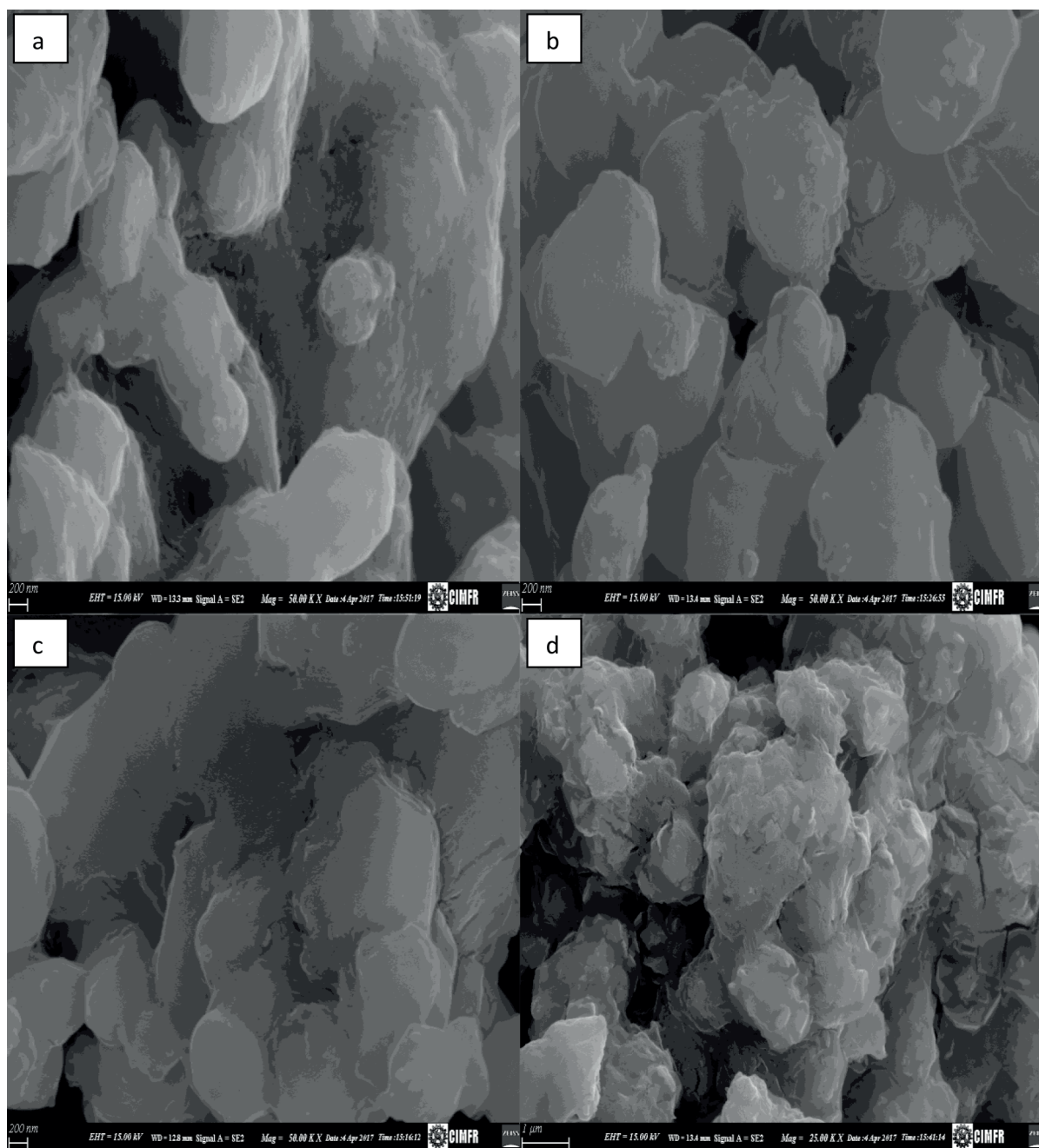


**Figure 4.** (a–d) SEM image of 35%  $K_2CO_3/CaO$  at different magnifications.

showed that the catalyst was porous, which raised the contact between the reactants and catalyst during transesterification reaction. This increased the catalyst capability and product of biodiesel. Agglomeration of the catalyst particle was extensively observed on the catalyst surface. Degirmenbasi et al. also reported agglomeration of catalyst particle in  $K_2CO_3/CaO$  catalyst by SEM study and some of the agglomerated particles were more than  $1 \mu m$  in dimension.<sup>5</sup> The spaces between the aggregates were  $1\text{--}5 \mu m$ . Such arrangements are more encouraging towards the access of triglycerides and methanol so that the basic sites

of the internal surface can also be utilized for transesterification. Guo et al. have reported the same explanation by using sodium silicate catalyst for the transesterification of soybean oil with methanol.<sup>29</sup>

Figure 5 shows the particle size distribution of (a) 35%  $K_2CO_3/CaO$  and (b)  $CaO$  catalyst. From the figure of 35%  $K_2CO_3/CaO$  catalyst, it is confirmed that a large part of the catalyst particles (90%) are less than  $114.41 \mu m$  and the rest of the particles (10%) are less than the  $8.69 \mu m$ . Most of the particles have big sizes; it is very easy to separate the catalyst from the reaction product after the transesterification reaction.

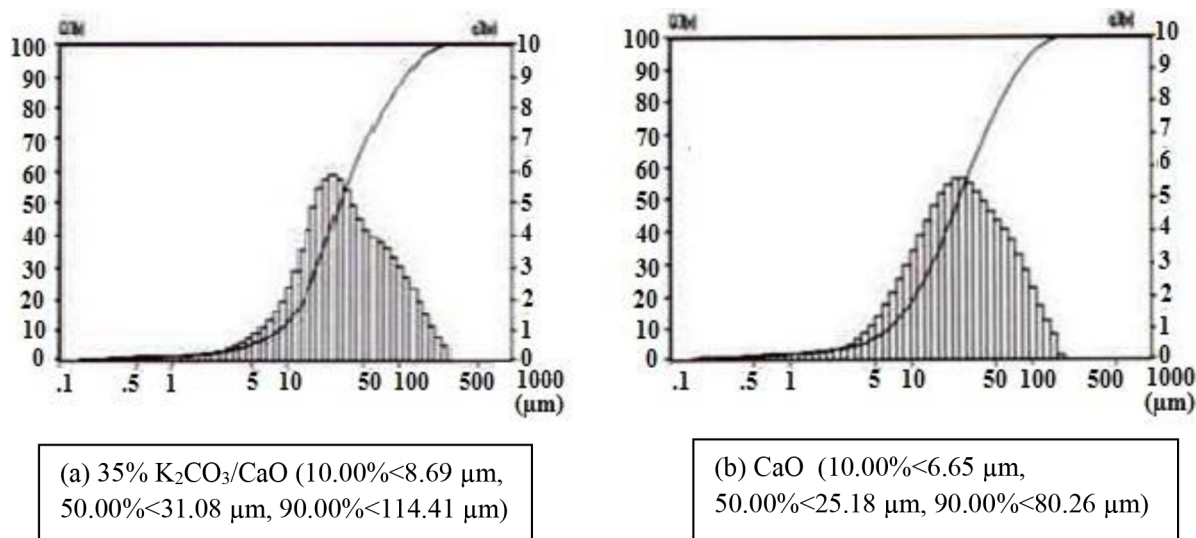


Figure 5. Particle size of (a) 35%  $K_2CO_3/CaO$  and (b)  $CaO$ .

The TGA graph of 35%  $K_2CO_3/CaO$  sample is depicted in Figure 6. The weight loss by dehydration, which occurs below  $350 \text{ }^\circ C$ , corresponded to the elimination of water molecules. A second weight loss was observed between  $400$  and  $600 \text{ }^\circ C$ , which was assigned slight decomposition of  $K_2CO_3$ . A third weight loss was detected in the range of  $700\text{--}900 \text{ }^\circ C$ , which may be due to the complete decomposition of  $K_2CO_3$ .

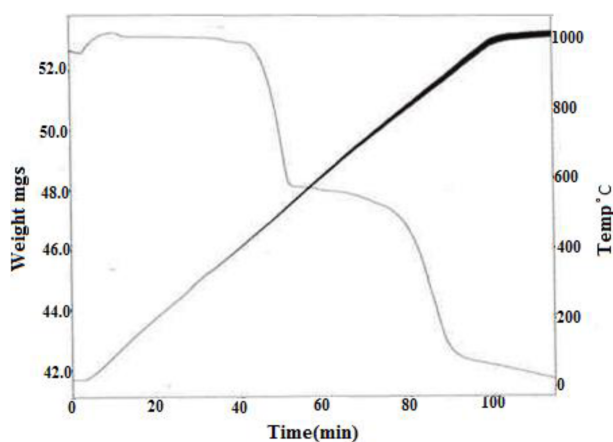


Figure 6. TGA graph of 35%  $K_2CO_3/CaO$ .

Based on the catalyst characterization results, we could finally conclude that the porosity, crystalline nature,  $K_2O$  species or  $Ca\text{--}O\text{--}K$  group, and  $K_2CO_3$  of the reported catalyst play a vital role for increasing conversion of jatropha oil to biodiesel.



## 2.1. Catalytic activity of pure CaO and K<sub>2</sub>CO<sub>3</sub>

The jatropha oil conversion is 23% using pure CaO and 72% using pure K<sub>2</sub>CO<sub>3</sub>. Both catalysts are calcined at 700 °C for 4 h. The reaction conditions are kept constant, i.e. reaction time, 3 h; methanol/oil molar ratio, 10:1; catalyst amount, 6 wt%; reaction temperature, 70 °C. The lower conversion using CaO may be due to the formation of soap. Endalew et al. reported only 18% FAME when the transesterification reaction of high FFA JCO was carried out using CaO with methanol under reaction conditions of 60 °C reaction temperature, 3 h of reaction time, 6:1 molar ratio of methanol to oil, 5 wt% catalyst (based on the amount of oil), and 300 revolutions per minutes (rpm).<sup>4</sup> Although CaO is a very active catalyst for the transesterification of low FFA oils. The formation of soap on the surface of CaO proceeds when the FFA in the oil is supposed to neutralize the Ca<sup>2+</sup> on the surface of the catalyst.<sup>19</sup> This soap inhibits the adsorption of methanol on the catalyst surface, which reduces the greater rate of the transesterification reaction. As a result of this, conversion is very low. However, in the case of pure K<sub>2</sub>CO<sub>3</sub>, the decrease in conversion could be due to the soap formation when 6 wt% catalyst was used. This was an indication of saponification of triglycerides as a secondary reaction with respect to transesterification. Previous studies showed that the excess alkali catalyst caused the saponification of triglycerides resulting in the formation of soap and in an increase in the viscosity of the reactants.<sup>30</sup> Baroi et al. also reported that saponification might be responsible for significantly lower conversion of jatropha oil to biodiesel when 7 wt% potassium carbonate was used instead of 6 wt% for transesterification of JCO having 2.86% FFA.<sup>31</sup> In our experiment, the decrease in conversion at 6 wt% K<sub>2</sub>CO<sub>3</sub> catalyst was due to the reduction of methyl ester content in the biodiesel product, which resulted probably from the increased solubility of soap into the biodiesel product. An excess amount of K<sub>2</sub>CO<sub>3</sub> catalyst (6 wt%) produces soap at long reaction time, i.e. 3 h, and gives lower conversion due to high FFA JCO. Under the same experimental conditions, no soap formation was observed during the transesterification reaction using K<sub>2</sub>CO<sub>3</sub>/CaO catalyst.

## 2.2. Influence of reaction parameters

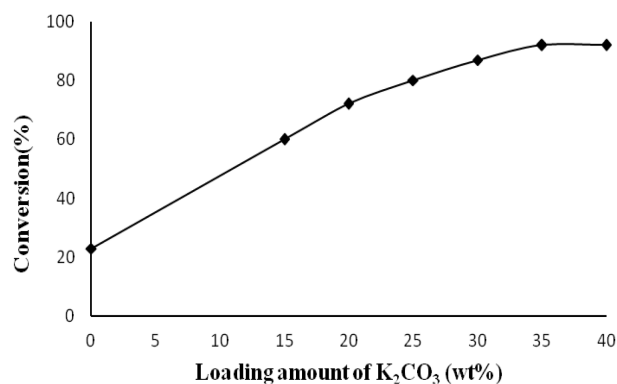
### 2.2.1. Influence of loading amount of K<sub>2</sub>CO<sub>3</sub> on the conversion

The influence of loading amount of K<sub>2</sub>CO<sub>3</sub> over CaO on transesterification of jatropha oil with methanol at 70 °C was examined with methanol to oil ratio of 10:1, 6% catalyst amount, 3 h reaction time, and 600 rpm mixing rate. The plot of different loading amount of K<sub>2</sub>CO<sub>3</sub> against conversion is shown in Figure 7. The reaction did not progress well with less than 35 wt% K<sub>2</sub>CO<sub>3</sub> loading amount. When the loading amount of K<sub>2</sub>CO<sub>3</sub> reached 35 wt%, conversion of 92% was observed. The reason was the presence of sufficient active sites on the catalyst. However, further increasing the amount of K<sub>2</sub>CO<sub>3</sub> appeared to be worthless and the conversion remained the same. Thus, the suitable loading amount of K<sub>2</sub>CO<sub>3</sub> on CaO for the present study was 35 wt%.

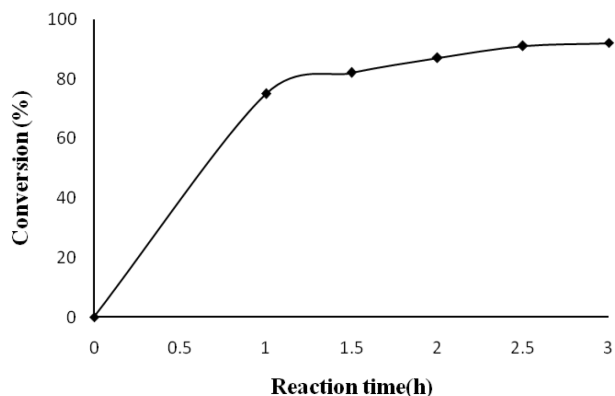
### 2.2.2. Influence of the reaction time on the conversion

Figure 8 illustrates the variation in reaction time on JCO transesterification with K<sub>2</sub>CO<sub>3</sub>/CaO catalyst amount (6 wt%), molar ratio of methanol/oil (10:1), at 70 °C. The triglyceride conversion to methyl ester was increased along with the reaction time and 92% conversion was achieved in 3 h. Leaching of K content to reaction mixture/biodiesel was measured by flame photometry. K content of biodiesel was found to be 517 ppm (0.052%). As the leaching of K content to biodiesel is quite low, the catalyst may be reused. However, it was further noted that when the reaction time was over 3 h the appearance of white gel in the product of methyl ester was slightly observed, which might be due to the presence of high FFA JCO. Moreover, 97.67% ± 1.7 of FAME was

found during the transesterification of canola oil with methanol using  $K_2CO_3$ /nano CaO in 8 h at 65 °C and 9:1 molar ratio of alcohol to oil.<sup>5</sup>



**Figure 7.** Influence of amount of  $K_2CO_3$  impregnation over CaO on jatropha oil transesterification.



**Figure 8.** Influence of reaction time on transesterification of jatropha oil using 35%  $K_2CO_3$ /CaO.

### 2.2.3. Influence of the reaction temperature on the conversion

Reaction temperature is an important factor that influences the reaction rate and conversion of JCO. Figure 9 demonstrates the variation in jatropha oil conversion at different reaction temperatures (60 °C to 100 °C) with methanol to oil molar ratio of 10:1, 6 wt% of  $K_2CO_3$ /CaO catalyst, and 3 h reaction time. The results signified that the conversion of jatropha oil to methyl ester first increased and then decreased with increasing reaction temperature. This could be due to accelerated saponification of the glycerides, which increased the viscosity of reactants and decreased the production of methyl ester. The soap formation in the reaction medium imparts difficulties in biodiesel and glycerol separation.<sup>9</sup> In addition, when temperature was over the boiling point of methanol, the evaporation of methanol started, which would restrain reactions on the three-phase interface. Therefore, the optimum temperature was 70 °C for the transesterification of JCO using  $K_2CO_3$ /CaO catalyst. Moreover, 70% yield of FAME was attained when the transesterification of JCO with methanol was carried out using KSF and Amberlyst 15 catalyst at 160 °C, 12:1 molar ratio of methanol to oil, 6 h reaction time, 5 wt% catalysts, and 300 rpm.<sup>32</sup>

### 2.2.4. Influence of the methanol/oil molar ratio on the conversion

The relationship between molar ratio of methanol to oil and conversion was studied using 35%  $K_2CO_3$ /CaO catalyst and the results are presented in Figure 10. When the ratio increased from 6:1 to 10:1, the conversion of jatropha oil moved progressively from 76% to 92%. Since jatropha oil was immiscible with methanol, excess methanol should be used to promote the reaction. The maximum conversion of 92% was achieved when the molar ratio was 10:1. A higher molar ratio over the stoichiometric value resulted in a high rate of biodiesel formation and a complete transesterification reaction.<sup>33</sup> A molar ratio over 10:1 had little effect on the conversion efficiency. Aluminum oxide-modified Mg-Zn is reported as a heterogeneous catalyst for the transesterification of crude jatropha oil with methanol;<sup>34</sup> 94% methyl ester is obtained under the reaction condition of 6 h reaction time, methanol to oil molar ratio of 11:1, 182 °C temperature, and 8.68% catalyst loading.

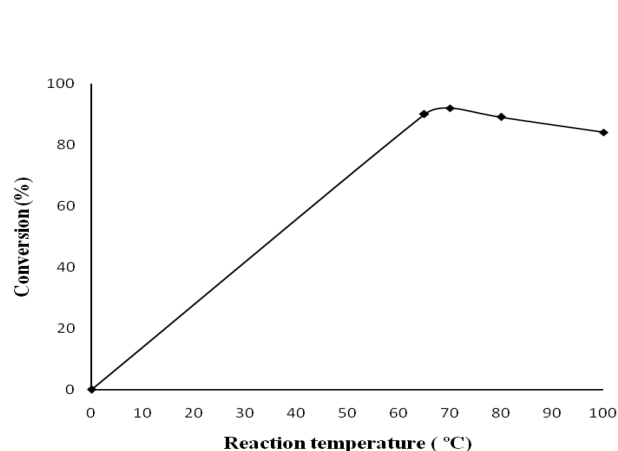


**Figure 9.** Influence of reaction temperature on transesterification of jatropha oil using 35%  $K_2CO_3/CaO$ .

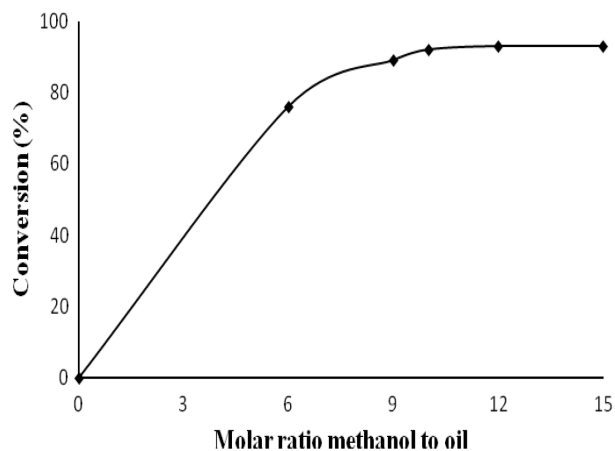


**Figure 10.** Influence of molar ratio on transesterification of jatropha oil using 35%  $K_2CO_3/CaO$ .

### 2.2.5. Influence of the catalyst amount on the conversion

Transesterification of jatropha oil in methanol (10:1 molar ratio) with 35%  $K_2CO_3/CaO$  was studied at 70 °C with varying catalyst amounts from 1 to 8 wt% (Figure 11). The conversion of *Jatropha curcas* oil using 35%  $K_2CO_3/CaO$  catalyst increased steadily with increasing the catalyst loading from 1 to 6 wt%. On the other hand, when the catalyst amount exceeded 6 wt%, the conversion to methyl ester was decreased. This may be due to resistance of mixing between the reactant, product, and solid catalyst. The result is consistent with the loading amount of solid base catalyst in the transesterification of soybean oil with methanol.<sup>35</sup> It was reported that the yield of biodiesel increased when the 30%  $KOH/Nd_2O_3$  catalyst amount increased from 1 to 6 wt% and decreased with increasing the catalyst amount beyond 6 wt%.

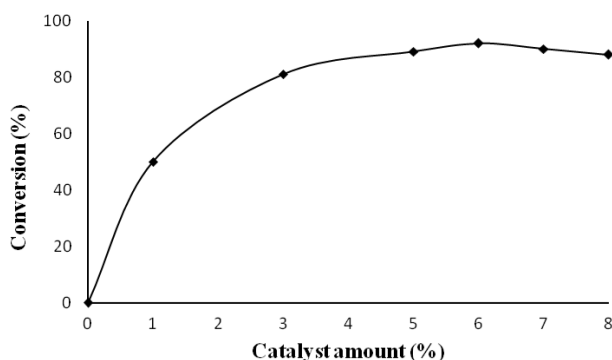


**Figure 11.** Influence of 35%  $K_2CO_3/CaO$  catalyst amount on transesterification of jatropha oil.

### 2.3. Conclusions

In the present work,  $K_2CO_3/CaO$  was reported as a heterogeneous solid base catalyst for the production of biodiesel from high FFA JCO. The 35%  $K_2CO_3/CaO$  catalyst was the optimum catalyst and gave the highest catalytic activity in the methanolysis of jatropha oil. The conversion of jatropha oil was found to be 92% as the reaction was carried out at 70 °C, with 10:1 molar ratio of methanol to oil, reaction time 3 h, and catalyst amount of 6 wt%. FTIR, XRD,  $CO_2$ -TPD, particle size analyzer, SEM study, true density,

and SA analyzer were employed for catalyst characterization. Catalyst characterizations through different analytical tools indicate that the porosity, crystalline structure,  $K_2O$  or  $Ca-O-K$  group,  $K_2CO_3$ , and isolated OH group present on the catalyst surface could be the active sites of the catalyst that could take part during the transesterification reaction.

### 3. Experimental

#### 3.1. Material section

JCO was collected from Rajasthan (Churu), India. The chemicals used for catalyst preparation such as  $K_2CO_3$ , CaO, and analytical reagent grade anhydrous methanol were procured from Sigma Aldrich Chemicals Pvt. Ltd., India. The purity of solvent and chemicals was 99%.  $CDCl_3$  and tetramethylsilane (TMS) used for  $^1H$  NMR analysis were purchased from Sigma Aldrich. HPLC grade methanol and all standards used for HPLC analysis were also purchased from Sigma Aldrich.

#### 3.2. Preparation of catalyst

The aqueous solution of  $K_2CO_3$  salt was added to the desired amount of metal oxide CaO, stirred vigorously for half an hour, and kept overnight for impregnation. After that water was removed in a water bath at  $100\text{ }^\circ\text{C}$  until dryness. Then the prepared catalyst was dried in an air oven at  $120\text{ }^\circ\text{C}$  for 16 h and finally the solid  $K_2CO_3/CaO$  catalyst was crushed and then calcined in a muffle furnace at  $700\text{ }^\circ\text{C}$  for 4 h. The molarity of  $K_2CO_3$  solution was 1.275 mol/L. The particle size of the catalyst after crushing was 1–114  $\mu\text{m}$ .

#### 3.3. Catalyst characterization

An Ultracycrometer 1000 (Quantachrome, USA) connected to a temperature controller (Julabo, USA) was used to determine the true density of catalysts by using helium as the probe gas.<sup>36</sup> This involved Archimedes' principle of fluid displacement and Boyle's law to determine the volume. The displaced fluid is a gas (helium gas), which can easily penetrate the pores.

Apparent density was determined using an AutoPore IV 9500 Mercury Porosimeter (Micromeritics, USA). From apparent density and true density, porosity can be determined.

The KBr pellet technique was incorporated to identify the FTIR spectra of samples and a DTGS detector was used. The FTIR spectra of  $K_2CO_3/CaO$  were recorded on a PerkinElmer FTIR system (Spectrum GX model) in the region of  $400\text{ cm}^{-1}$  to  $4000\text{ cm}^{-1}$  with  $2\text{ cm}^{-1}$  resolution. The ratio of catalyst sample to KBr was taken as 1:300. The spectrum of KBr was absorbed up to  $350\text{ cm}^{-1}$ . The mixture of catalyst sample and KBr was powdered in an agate mortar. Around 250 mg powder dried sample was taken in an evacuable die for making pellets using 10,000 kg hydraulic pressure for 2 to 3 min. Each spectrum was obtained in transmission mode over 50 scans. Due to the large scan, a fast and accurate FTIR spectrum was obtained with a much better signal to noise ratio. Background spectra were collected before every sampling. KBr was previously air oven-dried to avoid interferences due to the presence of water. Finally, the FTIR spectrum was plotted  $\text{cm}^{-1}$  versus transmittance or absorbance.

The BET SA of the calcined catalysts was determined using a Tristar 3000 SA analyzer (Micromeritics, USA). The SA of the samples was measured by using nitrogen as adsorbate gas at  $-196\text{ }^\circ\text{C}$  (liquid nitrogen temp.). The BET SA was determined from adsorption of nitrogen onto the catalyst surface in a liquid nitrogen bath. Prior to the experiment, all the samples are degassed for 3 h at  $150\text{ }^\circ\text{C}$  to remove the impurity present

in the catalysts. The BET SA was calculated from the adsorption of nitrogen in the relative pressure range of 0.05 to 0.3.

XRD measurement was done with the help of a D-8 advanced (M/S Bruker AXS, Germany) X-ray diffractometer with Cu K $\alpha$  radiation ( $\lambda_1 = 1.5406 \text{ \AA}$ ,  $\lambda_2 = 1.5444 \text{ \AA}$ ). Spectra were collected over a  $2\theta$  range of  $10\text{--}75^\circ$  with step scan mode (step size of  $0.02^\circ/\text{step}$ , scan speed of  $1 \text{ s/step}$ ). The XRD phases were identified by search match procedure with the help of the JCPDS databank.

A laser-based particle analyzer instrument (Fritsch GmbH Germany) was used to determine the size of the catalyst sample with resolution 62 channels (9 mm/254 mm). Data were recorded over a measuring range of  $0.10[\mu\text{m}]\text{--}670.07[\mu\text{m}]$  at 20 scans.

CO<sub>2</sub>-TPD was executed using an Auto Chem 2910 (Micromeritics, USA) instrument for studying the basicity of the catalysts. First 0.04 g of powdered K<sub>2</sub>CO<sub>3</sub>/CaO sample was degassed at  $120^\circ\text{C}$  for 1 h with helium flow rate of 50 mL/min. Then the sample was cooled to  $45^\circ\text{C}$  and at this temperature the gas flow was changed. Then adsorption of CO<sub>2</sub> was carried out using a mixture of 2% CO<sub>2</sub> in He for 45 min. Helium gas (purge gas) flow was started again at the same temperature to remove loosely adsorbed carbon dioxide molecules from the catalyst surface. Finally, the sample was heated at a flow rate of  $10^\circ\text{C}/\text{min}$  up to  $975^\circ\text{C}$  using He as a carrier gas to desorb CO<sub>2</sub>.

SEM analysis of the catalyst was carried out on a ZEISS EVO series scanning electron microscope model EVO 50. The K<sub>2</sub>CO<sub>3</sub>/CaO catalyst was coated with a gold sputtering unit. The equipment was accelerated at 20.0 kV to estimate the particle size and shape of the catalyst.

Thermal decomposition of the K<sub>2</sub>CO<sub>3</sub>/CaO sample was calculated by thermogravimetric analyzer STA 449 F3 Jupiter (Netzsch, Germany) under argon flow at a  $10^\circ\text{C}/\text{min}$  heating rate up to  $800^\circ\text{C}$ .

### 3.4. Transesterification reaction

Low quality jatropha oil was used in the transesterification reaction. The FFA of jatropha oil was found to be 5.5%. It was measured by titration. It is just half of an acid value. Around 2 g of oil was taken in a 250 mL conical flask. Then 25 mL of ethanol was added to the flask and 1 mL of naphthalene indicator was added to the flask. Then it was slightly agitated to completely dissolve the oil in the solvent. It was faintly warmed and titrated with 0.1 N KOH solutions. Acid value is determined by  $\text{Acid value (mg KOH/g)} = 56.1 \times V \times N/W$ , where V is the volume of standard 0.1 N KOH solution, N is the normality of potassium hydroxide, and W is the weight of oil in grams. Gas chromatography (GC-FID) was used to measure the fatty acid composition of oil. The fatty acid composition consisted of palmitic acid (C16:0) 23.2%, palmitoleic acid (C16:1) 0.8%, stearic acid (C18:0) 10.9%, oleic acid (C18:1) 52%, linoleic acid (C18:2) 9.0%, and arachidic acid (C20:0) 0.4%, according to GC-1000. Then 50 mL of JCO and the desired amount of catalyst were taken in a 250 mL two-necked glass flask equipped with a temperature controller with a magnetic stirrer. The reaction was carried out with a water cooled reflux condenser to check the evaporation loss of methanol so that it cannot be removed from the reaction mixture even if the temperature was maintained above the boiling point of methanol. Then the required amount of methanol was added to the flask. The mixture was stirred vigorously and refluxed at  $70^\circ\text{C}$  for 3 h. After the reaction, the reaction mixture was separated from the catalyst particles by centrifugation. Then the reaction product was kept for 24 h. The product was separated into two layers, i.e. the upper layer is the biodiesel layer and the lower layer is the glycerol layer. Then the biodiesel product was distilled at  $170\text{--}190^\circ\text{C}$  and 4 mg pressure to get pure biodiesel. This pure biodiesel was used for further analysis.

The transesterification reaction was monitored by thin layer chromatography (TLC), <sup>1</sup>H NMR spec-

trosopy, and HPLC analysis. For the TLC method, qualitative analysis of the reaction product was performed. The solvent system used for TLC was hexane:diethyl ether:acetic acid in the proportions of 85:15:1. A Bruker 300 MHz (Bruker DPX-300, Rheinstetten, Germany) spectrometer was used for  $^1\text{H}$  NMR analysis where  $\text{CDCl}_3$  is used as a solvent and tetramethylsilane (TMS) as the standard reference. The methyl esters present in the product of the transesterification of jatropha oil were analyzed using HPLC (PerkinElmer Series 200) with a refractive index detector (Shodex RI 71). A sphere-5 C-18 column (PerkinElmer Brownlee column,  $220 \times 4.6$  mm with  $5 \mu\text{m}$  particle size) at  $40^\circ\text{C}$  was used for separation of the components with 1 mL/min flow rate of methanol as carrier solvent.

### 3.5. Analysis of methyl esters in biodiesel by analytical method

TLC was used to monitor the progress of the transesterification reaction. TLC of jatropha oil and jatropha oil methyl ester (JOME) is shown in Figure 12. The progress of the reaction was observed by the appearance of a methyl ester spot and disappearance of the jatropha oil spot on the TLC plate.



Crude oil      Crude Biodiesel

**Figure 12.** TLC for monitoring the transesterification of jatropha oil.

$^1\text{H}$  NMR analysis was used to measure the jatropha oil conversion in the transesterification reaction. The  $^1\text{H}$  NMR spectra of jatropha oil and JOME using  $\text{K}_2\text{CO}_3/\text{CaO}$  are shown in Figures 13 and 14, respectively. The conversion of jatropha oil to methyl ester was calculated using the following relation:

$$C = 100 \times \frac{2A_{ME}}{3A_{\alpha-CH_2}},$$

where  $C$  = conversion of triglycerides (vegetable oil) to methyl ester;  $A_{ME}$  = integration value of the protons of methoxy groups of the methyl ester;  $A_{\alpha-CH_2}$  = integration value of the methylene protons. The factors 2 and 3 indicate the methylene carbon possesses two protons and the methoxy carbon possesses three protons, respectively. The multiplet peaks at 4.2–4.4 ppm in the  $^1\text{H}$  NMR spectra of jatropha oil are due to glyceridic protons (Figure 13). In the  $^1\text{H}$  NMR spectrum of the biodiesel sample, the disappearance of glyceridic protons (4.2–4.4 ppm) and appearance of a new peak at 3.68 ppm due to  $-\text{OCH}_3$  protons indicated the conversion of oil to biodiesel.

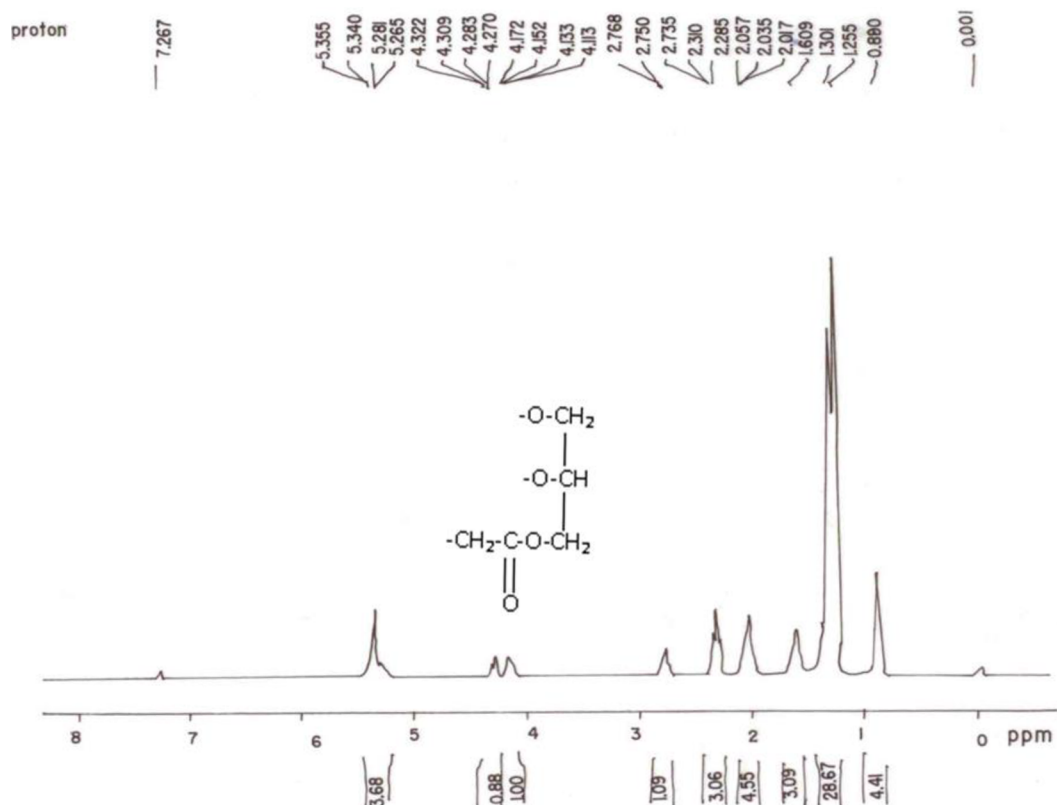


Figure 13.  $^1H$  NMR spectrum of jatropha oil.

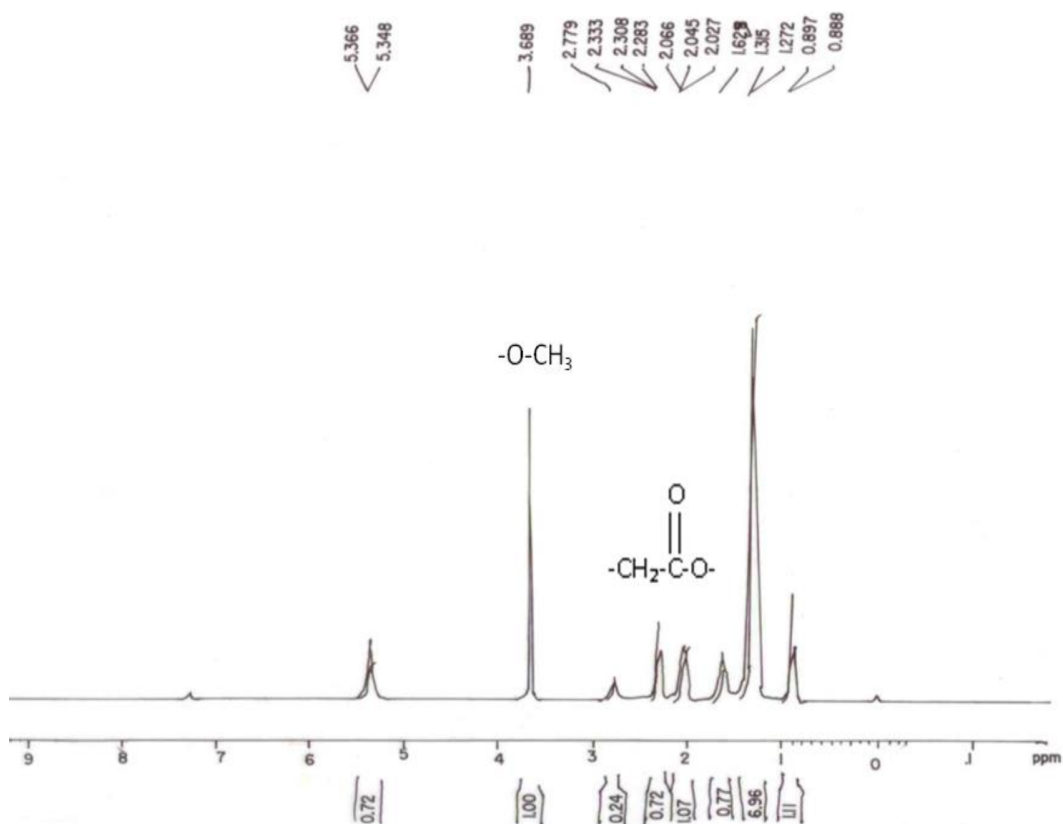


Figure 14.  $^1H$  NMR spectrum of jatropha biodiesel using  $K_2CO_3/CaO$ .

The HPLC chromatogram of JOME using  $K_2CO_3/CaO$  catalyst is shown in Figure 15, which indicates the presence of methyl linolenate (MeLn), methyl oleate (MeO), methyl palmitate (MeP), and methyl stearate (MeS). Each component was quantified by comparing the peak areas with their corresponding standards. This analytical method was used for cross checking of the biodiesel product.

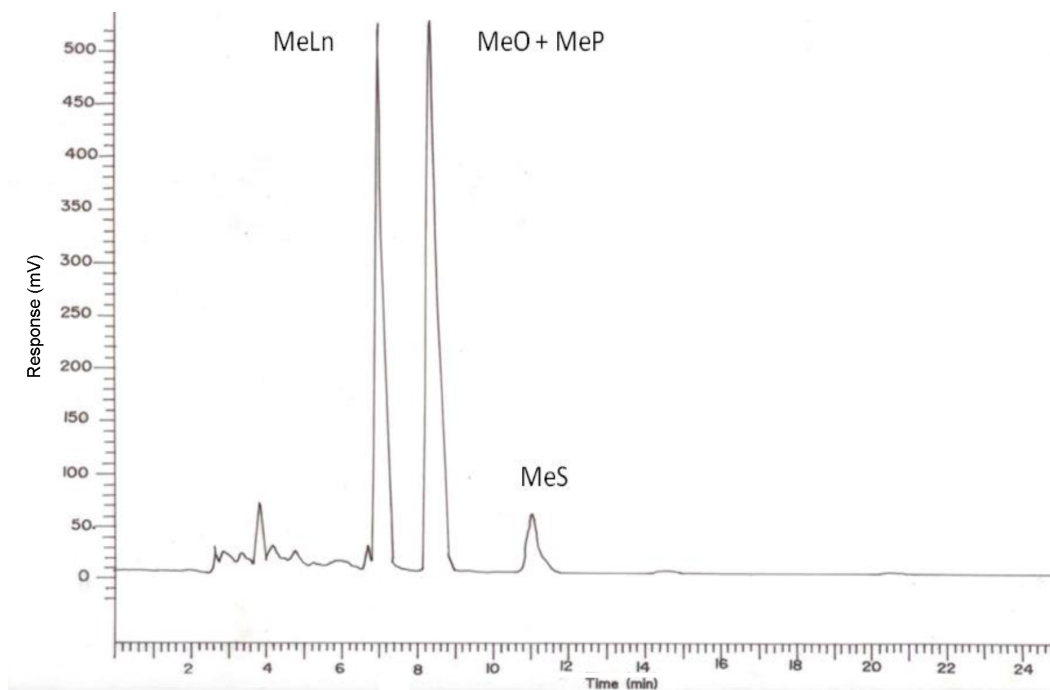


Figure 15. HPLC chromatogram of biodiesel using  $K_2CO_3/CaO$ .

### Acknowledgments

The authors thank the Director, Central Institute of Mining and Fuel Research (CIMFR), Dhanbad, CSIR (Govt. of India), for financial support to carry out the present experimental work. The authors also thank Dr KMP Singh, Coal preparation and Carbonization Research Group, for analyzing the SEM of the reported catalyst.

### References

1. Srivastava, A.; Prasad, R. *Renew. Sust. Energ. Rev.* **2000**, *4*, 111-133.
2. Martinez-Herrera, J.; Siddhuraju, P.; Francis, G.; Davila-Ortiz, G.; Becker, K. *Food Chem.* **2006**, *96*, 9680-9689.
3. Meher, L. C.; Dharmagadda, V. S. S.; Naik, S. N. *Bioresour. Technol.* **2006**, *97*, 1392-1397.
4. Endalew, A. K.; Kiros, Y.; Zanzi, R. *Energy* **2011**, *36*, 2693-2700.
5. Degirmenbasi, N.; Coskun, S.; Boz, N.; Kalyon, D. M. *Fuel* **2015**, *153*, 620-627.
6. Zhu, H.; Wu, Z.; Chen, Y.; Zhang, P.; Duan, S.; Liu, X.; Mao, Z. *Chin. J. Catal.* **2006**, *27*, 391-396.
7. Kaur, M.; Ali, A. *Renew. Energ.* **2011**, *36*, 2866-2871.
8. Taufiq-Yap, Y. H.; Lee, H. V.; Yunus, R.; Juan, J. C. *Chem. Eng. J.* **2011**, *178*, 342-347.
9. Lee, H. V.; Yunus, R.; Juan, J. C.; Taufiq-Yap, Y. H. *Fuel Process. Technol.* **2011**, *92*, 2420-2428.



10. Taufiq-Yap, Y. H.; Lee, H. V.; Hussein, M. Z.; Yunus, R. *Biomass Bioenergy* **2011**, *35*, 827-834.
11. Yaakob, Z.; Sukarman, I. S. B.; Narayanan, B.; Abdullah, S. R. S.; Ismail, M. *Bioresour. Technol.* **2012**, *104*, 695-700.
12. Arzamendi, G.; Arguinarena, E.; Campo, I.; Zabala, S.; Gandia, L. M. *Catal. Today* **2008**, *133-135*, 305-313.
13. Wen, L.; Wang, Y.; Lu, D.; Hu, S.; Han, H. *Fuel* **2010**, *89*, 2267-2271.
14. Granados, M. L.; Poves, M. D. Z.; Alonso, D. M.; Mariscal, R.; Galisteo, F. C.; Moreno-Tost, R.; Santamaria, J.; Fierro, J. L. G. *Appl. Catal. B: Environ.* **2007**, *73*, 317-326.
15. Vujcic, D.; Comic, D.; Zarubica, A.; Micic, R.; Boskovic, G. *Fuel* **2010**, *89*, 2054-2061.
16. Lukic, I.; Krstic, J.; Jovanovic, D.; Skala, D. *Bioresour. Technol.* **2009**, *100*, 4690-4696.
17. Kouzu, M.; Kasuno, T.; Tajika, M.; Yamanaka, S.; Hidaka, J. *Appl. Catal. A: Gen.* **2008**, *334*, 357-365.
18. Encinar, J. M.; Gonzalez, J. F.; Pardal, A.; Martinez, G. *Fuel Process. Technol.* **2010**, *91*, 1530-1536.
19. Kouzu, M.; Kasuno, T.; Tajika, M.; Sugimoto, Y.; Yamanaka, S.; Hidaka, J. *Fuel* **2008**, *87*, 2798-2806.
20. Liang, X.; Gao, S.; Wu, H.; Yang, J. *Fuel Process. Technol.* **2009**, *90*, 701-704.
21. Liu, X.; He, H.; Wang, Y.; Zhu, S.; Piao, X. *Fuel* **2008**, *87*, 216-221.
22. Ebiura, T.; Echizen, T.; Ishikawa, A.; Murai, K.; Baba, T. *Appl. Catal. A: Gen.* **2005**, *283*, 111-116.
23. Pojananukij, N.; Runruksa, N.; Neramittagapong, S.; Neramittagapong, A. *International Transaction Journal of Engineering, Management, & Applied Sciences & Technologies* **2010**, *5*, 78-86.
24. Mutreja, V.; Singh, S.; Ali, A. *Renew. Energy* **2011**, *36*, 2253-2258.
25. Boey, P. L.; Maniam, G. P.; Hamid, S. A. *Bioresour. Technol.* **2009**, *100*, 6362-6368.
26. Babu, N. S.; Sree, R.; Sai Prasad, P. S.; Lingaiah, N. *Energy Fuels* **2008**, *22*, 1965-1971.
27. Shumaker, J. L.; Crofcheck, C.; Tackett, S. A.; Santillan-Jimenez, E.; Morgan, T.; Ji, Y.; Crocker, M.; Toops, T. *J. Appl. Catal. B: Environ.* **2008**, *82*, 120-130.
28. Cosimo, J. I. D.; Diez, V. K.; Xu, M.; Iglesia, E.; Apesteguia, C. R. *J. Catal.* **1998**, *178*, 499-510.
29. Guo, F.; Peng, Z. G.; Dia, J. Y.; Xiu, Z. L. *Fuel Process. Technol.* **2010**, *91*, 322-328.
30. Rashid, U.; Anwar, F. *Energy Fuels* **2008**, *22*, 1306-1312.
31. Baroi, C.; Yanful, E. K.; Bergougnou, M. A. *Int. J. Chem. React. Eng.* **2009**, *7*, 1-16.
32. Zanette, A. F.; Barella, R. A.; Pergher, S. B. C.; Treichel, H.; Oliveira, D.; Mazutti, M. A.; Silva, E. A.; Oliveira, J. V. *Renew. Energy* **2011**, *36*, 726-731.
33. Leung, D. Y. C.; Guo, Y. *Fuel Process. Technol.* **2006**, *87*, 883-890.
34. Olutoye, M. A.; Hameed, B. H. *Bioresour. Technol.* **2011**, *102*, 6392-6398.
35. Li, Y.; Qiu, F.; Yang, D.; Li, X.; Sun, P. *Biomass Bioenergy* **2011**, *35*, 2787-2795.
36. Saha, S.; Sharma, B. K.; Kumar, S.; Sahu, G.; Badhe, Y. P.; Tambe, S. S.; Kulkarni, B. D. *Fuel* **2007**, *86*, 1594-1600.